멤브레인(Membrane Journal)
Vol.12, No.2, June, 2002, 107-119

기체분리용 고투과선택성 탄소-실리카막

박 호 범 · 이 영 무†

한양대학교 응용화학공학부 국가지정분리막연구실
(2002년 5월 27일 접수, 2002년 6월 14일 채택)

High Permeability, High Selectivity Carbon-Silica Membranes for Gas Separation

Ho Bum Park and Young Moo Lee†

National Research Laboratory for Membranes, School of Chemical Engineering, College of Engineering, Hanyang University, Seoul 133-791, Korea
(Received May 27, Accepted June 14, 2002)

요 약 : 이번 연구에서 효율적인 기체분리를 위한 탄소-실리카($C\text{-}SiO_2$) 분리막이 방향족 이미드 블록과 실록산 블록으로 구성된 공중합체의 비활성분위기에서의 열분해를 통해 제조되었다. 이 탄소-실리카 기체분리막은 비교적 작은 크기의 기체분리, 즉 He/N_2, O_2/N_2 그리고 CO_2/N_2의 분리에 있어 매우 뛰어난 기체선택도를 나타내었다. 두 상을 가진 공중합체의 열분해는 600도, 800도 그리고 1000도의 최종열분해온도로서 수행되었으며, 이러한 두 상으로 이루어진 전구체는 탄소막의 제조에 처음으로 보고되었다. 이러한 전구체는 두 상의 조성 및 같은 조성에서 중합방법의 차이에 의해 형성되는 모폴로지의 변화가 최종 탄소-실리카막의 기체분리특성에 미치는 영향을 살피기 위해 제조되었다. 이러한 탄소-실리카분리막은 2.6-3.64Å의 동력학적 반경을 가진 작은 기체분자(헬륨, 산소, 질소, 이산화탄소)들을 사용한 기체투과실험에서, 탄소-실라카 분리막은 높은 투과도와 함께 뛰어난 분자체 효과를 보였다. 게다가 탄소-실리카분리막의 기체분리특성은 사용한 고분자 전구체의 기체분리특성과 매우 유사하며, 이것은 열적으로 안정한 두상의 사용으로 전구체의 초기 모폴로지가 열처리 후에도 상당히 유지되었기 때문이다. 현재의 연구는 탄소막 전구체의 초기의 모폴로지가 최종 탄소막의 분리특성 및 미세구조에 결정적인 영향을 미침을 암시한다.

Abstract : Carbon-silica ($C\text{-}SiO_2$) membranes can be easily prepared by the pyrolysis of two-phase copolymers containing an aromatic imide block and a siloxane block and remarkably high permselectivities of He/N_2, O_2/N_2, and CO_2/N_2. The pyrolysis of the imide-siloxane block copolymers was carried out at different final temperatures, 600°C, 800°C, and 1000°C under an inert atmosphere, and is the first reported case of the precursors being used for the preparation of carbon membrane. The polymeric precursors were synthesized in a wide range of siloxane content and different final morphology, and the pyrolyzed membranes were tested with a high vacuum time-lag method at 25°C and 76cmHg of feed pressure. In experiments with He, CO_2, O_2, and N_2, the membranes were found to have good O_2/N_2 selectivity up to 32.2 and O_2 permeability on the order of 10^{-8} $cm^3(STP)cm/cm^2seccmHg$.

Keywords : Gas separations; Carbon-silica membrane; Membrane preparation; Two-phase polymer

†주저자(e-mail : ymlee@hanyang.ac.kr)

1. Introduction

Membrane technology has been presently established at several industrial processes and application. Particularly, gas separation (GS) is a relatively young technology and accounts for about US$230 million per year, but is growing fast with a rate higher than 15% a year[1]. The chemical industry is a growing field in the application of membranes, which, however, often requires membrane materials with exceptional stability. During the last decade inorganic materials such as zeolites, porous silicas and pyrolytic carbon molecular sieves have been developed with exciting unmatched selectivities for certain gas mixtures and some of the inorganic membranes described in the scientific literature seem to be on the brink of commercialization. The current market for inorganic membranes for gas separation is extremely small. One of the few commercial applications is small scale palladium membrane systems to produce ultrapure hydrogen for specialized applications. As present, it is not expected that the market share of inorganic membranes will increase significantly in the near future. The main obstacle is their high price and some principles difficulties during reproducible large-scale production.

The peculiar ability of the chemical element carbon to combine with itself and other chemical elements in different ways is the basis of organic and inorganic chemistry and of life. The chemical versatility in carbon also gives rise to various structural forms of carbon in the solid state. The materials include crystalline forms of carbon such as diamond, graphite, fullerences[2] and carbines, amorphous carbon films, carbon nanoparticles including carbon nanotubes[3], engineering carbons with more or less disordered microstructures based on that of graphite. Among the various types of carbons, porous carbonaceous materials are widely utilized for applications such as water and air purification, gas separation, catalysis, and energy storage[4,5]. In the field of gas separation, the flat-type membranes prepared from these porous carbons, including molecular sieve carbon membranes (MSCM), nanoporous carbon membranes (NPC)[6], and adsorption-selective carbon membranes (ASCM)[7], have been extensively studied for the last decades. The early development of the carbon membranes has utilized prior understanding of the nature of microporous carbon-molecular sieving, selective-adsorption, and catalytic reactions of small molecules. Most carbon membranes are typically obtained via carbonization of natural or synthetic polymeric precursors such as cellulose acetate[8], poly(vinylidene chloride)[9], poly (furfuryl alcohol)[10], phenolic resins[11,12] and polyimides[13-15].

The key-factors determining the microstructure and gas separation properties of the carbon membranes are the choice of polymeric precursor and the pyrolysis condition. The polymeric precursors have been usually chosen as materials that generate carbon in 25-50% or more mass yields on the basis of the original mass of the precursor after the pyrolysis. Up to date, the research work on carbon membranes has been mainly focused on the pyrolysis conditions and easy fabrication methods using mostly homopolymers. The separation of small gas molecules (<4 Å) by means of the carbon membranes should be effectively achieved via a molecular sieving mechanism. To control the micropores with sizes close to the dimensions of permanent gases, the pyrolysis conditions such as the pyrolysis temperature, the heating rate, and the pyrolysis atmosphere can be very important, but suffering from sacrificing permeating fluxes in order to achieve the high permselectivity.

Carbon is perhaps the most thermo-chemically stable material but is very susceptible to oxidation, which is an obvious drawback to the easy and reproducible fabrication of the carbon matrix. Therefore combining carbon with silicon, which is the neighbor of carbon in the fourth column of the periodic table, seems to be a natural choice for the next step in expanding the modern molecular separation science and technology.

Central to our study was the development of a new type of carbonaceous membranes using self-organized polymeric nanostructured materials (SOPNMs) such as block copolymers that consisted of two thermostable blocks, only differentiating carbon density. Based on SOPNMs, peculiar spatial regulation of these precursors after carbonization process made it possible to control the structure of carbonaceous materials at a nonometer level by changing either the size or the shape of the nanospace in SOPNMs. In the present

Table 1. The Sample Designation and the Composition of PIS

Class I	PMDA (mmol)	ODA (mmol)	PDMS (mmol)	Volume fraction of siloxane moiety
PIS I	10	9.8	0.2	0.06
PIS II	10	9.0	1.0	0.27
PIS III	10	8.0	2.0	0.46
Class II	BTDA (mmol)	ODA (mmol)	PDMS (mmol)	
r-/*b*-PIS	10	9.0	1.0	0.34

study, the use of thermally stable components in all building blocks distinguished our approach from the conventional carbonization methods[16-18].

2. Experimental Section

2.1. Materials

Pyromellitic dianhydride (PMDA), benzophenone-3, 3'4,4'-tetracarboxylic acid dianhydride (BTDA) and 4,4'-oxydianiline (ODA) were obtained from Tokyo Kasei Co., Inc., Tokyo, Japan and used without further purification. Amine-terminated polydimethylsiloxane (PDMS) was kindly donated by Shinetsu Co., Inc., Tokyo, Japan and used after drying in vacuum oven at 90°C. N-methylpyrrolidinone (NMP) and tetrahydrofuran (THF) were obtained from Aldrich Chemical Co. Inc. WI, U.S.A. and dried over 5Å molecular sieves overnight.

2.2. Preparation of Carbon-Silica Precursors

Poly(imide siloxane)s (PISs) used as carbon-silica (C-SiO_2) membranes were prepared by one-step or two-step polymerization. That is, in this study, five copolymers of two classes were designed and prepared using two 'building blocks' that consists of a rigid block and a flexible block. The rigid blocks consist of PMDA or BTDA and ODA whilst the flexible block is PDMS. In class I (PIS I, PIS II and PIS III), three copolymers having the different volume fraction of siloxane moiety were synthesized, denoted as class I-1, class I-2 and class I-3 by the order of the siloxane volume fraction. In class II (*r*-PIS, *b*-PIS), two copolymer having a different geometry-random and block at a constant siloxane volume fraction were prepared, denoted as class II-*r* and class II-*b*, respectively. The chemical composition of PIS samples prepared in this work is summarized in Table 1.

In the preparation of class I samples, powders of PMDA (10 mmol) were added dropwise to the THF solution of PDMS (0.2, 1.0 and 2.0 mmol, respectively) under a nitrogen atmosphere, and then the solutions of mixtures stirred for 1h. The reaction mixtures were added dropwise to NMP solutions of ODA (9.8, 9.0 and 8.0 mmol, respectively). The resulting solutions were stirred at room temperature for 6h. Resultantly, homogeneous yellowish siloxane-containing poly(amic acid) (PAA) solutions were then obtained. The solid concentration of PAAs was kept about 10 wt%. The PAA solutions were cast onto a glass plate and then thermally imidized at 100°C for 1h, 200°C for 1h, 300°C for 1h and 350°C for 1h under a vacuum so as to produce strong, flexible and dense 20-30 μm films.

In the preparation of class II samples, for *b*-PIS sample, powders of BTDA (2 g, 1 mol) were added dropwise to THF solution of PDMS (0.112 g, 1 mmol) under nitrogen atmosphere at room temperature, and then the solution of mixture was stirred for 5 h. Then, the reaction mixture was added dropwise to NMP solution of ODA (1.218 g, 9 m mol). The resulting solution was stirred at room temperature for 6 h under nitrogen atmosphere. Thermal imidization procedure is the same as mentioned above. To prepare *r*-PIS sample, powders of BTDA were reacted with THF/NMP mixture solution of PDMS and ODA, simultaneously. The reaction mixture was stirred for 12 h under nitrogen atmosphere at room temperature. The thermal imidization procedure and film formation was the same as that of *b*-PIS. These PIS samples were stored at dessicator in order to eliminate the effect of humidity.

2.3. Inert Pyrolysis of PIS Films

Pyrolytic carbon membranes including molecular

sieving carbons or nanoporous carbons can be carefully made from the inert or vacuum pyrolysis of natural and synthetic polymers. Before starting a pyrolysis trial, the free standing PIS films were rinsed with deionized water and stored at 120°C under a vacuum oven until any residual solvent and any dusts were thoroughly eliminated. After the pretreatment, the PIS films were then placed in a muffle furnace equipped with an automatic temperature controller.

The PIS films were pyrolyzed under an Ar flow in a quartz tube furnace supported on an alumina holder plate. The Ar flow was precisely controlled by a mass flow controller (MKS Instruments, MASS-FLO®, MA, U.S.A.). A 4.5 cm ID, 70 cm long quartz tube with a glass end cap was used for the pyrolysis in a muffle furnace equipped with four heating elements to minimize the axial and radial temperature gradients. A distance of an effective heating zone was 30 cm and a maximum heating temperature was 1500°C.

A pyrolysis protocol was followed thoroughly to obtain reproducible gas permeation properties of the final carbon-silica membranes. The pyrolysis protocol applied in this work was predetermined by the result obtained from thermogravimetric analysis coupled with mass spectroscopy (TGA-MS) as reported in our previous works[19]. Prior to heating the furnace, the PIS films were kept for 1h under an inert purge in order to stabilize the atmosphere and to remove any oxidant in a quartz tube.

The heating rate used in the initial stage was 10°C/min from room temperature to 400°C. The heating rate was slowed to 3°C/min until the temperature reached up to 600°C. Then the PIS films were kept at 600°C for 2 h (denoted as PIS-600). From 600°C, the heating rate was again ramped to 3°C/min up to 800°C. The pyrolyzed PIS films were held at 800°C for 2h (denoted as PIS-800). Finally, from 800°C, the heating rate was increased to 3°C/min until the temperature reached up to 1000°C and the resultant PIS films were held at this temperature for 2h (denoted as PIS-1000). The furnace was allowed to cool slowly down to room temperature. The final pyrolytic carbon-silica membranes were taken from the quartz tube and then stored in a dessicator filled with dry silica gel to minimize the humidity effect.

2.4. Gas Permeation Experiments

Gas permeation measurements were conducted using the high-vacuum time-lag method at a feed pressure of 760 torr and a feed temperature of 25°C. Before the gas permeation measurements, both the feed and the permeate sides were thoroughly evacuated at below 10^{-5} torr. The pressure rise versus time transient of the permeate side equipped with a pressure transducer (MKS Baratron type 146) was recorded to a desktop computer through a RS-232 cable. The linear slope of the pressure rise versus time provides the permeation rates of permanent gases. The permeability coefficient for a permanent gas is determined by multiplying the permeation rate by the membrane thickness and can be expressed as follows:

$$P = \frac{dp}{dt}\left(\frac{VT_0L}{p_0T\Delta pA}\right) \quad (1)$$

where P is the permeability represented in Barrer, dp/dt is the rate of the pressure rise under the steady state, V (cm^3) is the downstream volume, L (cm) is the membrane thickness, Δp (cmHg) is the pressure difference of both sides, T (K) is the measurement temperature, A (cm^2) is the effective area of the membrane, and p_0 and T_0 are the standard pressure and temperature, respectively. Permselectivity defined in this study was the ratio of permeability of the selected gases over that of nitrogen.

3. Membrane Transport and Selective Phenomena

The mechanisms by which various components in a gaseous feed stream are transported through the membrane material determine the separation properties of the membrane. Seven different mechanisms may be identified in the transport of gases across a porous material: viscous flow, Knudsen diffusion, transition flow, surface diffusion, capillary condensation, micropore diffusion and molecular sieving. The contribution of the different mechanisms is dependent on the properties of the membranes and the operating conditions. The actual transport mechanism is determined by: gas properties (molecular weight, a collision diameter and adsorption characteristics), the pore size,

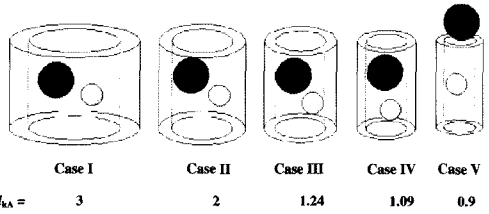

Fig. 1. Different pore size regimes related to molecular size, for description see text (r is the pore radius and d_{kA} is the kinetic diameter of gas A).

pore size distribution of the membrane and pore surface properties. Here, we review only the micropore diffusion occurring in the molecular sieving membranes such as pyrolytic carbon membrane and Zeolite.

Transport mechanism called micropore diffusion takes place in membranes with a pore diameter smaller than 2 nm. In a microporous system, a few different cases can be distinguished according to the nature of the molecular-wall interactions. The transport behavior will change as the ratio of the diameters of the gas molecule and the pore changes. This is often accompanied by change in adsorption and/or mobility energy. An overview of a number of typical cases can be described and is given in Fig. 1. The effect of a decreasing pore size on the transport mechanism is given below:

Case I: This is near the boundary between the meso- and micropore region. In the central region of the pore, the gas molecules can move freely (Knudsen diffusion). Adsorbed molecules will diffuse along the surface, where the heat of adsorption is enhanced by the opposing wall.

Case II: The molecules in the center of the pore still behave Knudsen-like and can pass each other, but nevertheless are not really free anymore. The heat of sorption increases and the mobility of large molecules compared to the pore size decreases.

Case III: The gases cannot pass any more and differences in permeance are largely determined by differences in sorption characteristics and mobility.

Case IV: When the effective pore diameter $d_{eff} < d_{kA} + d_{kB}$, both gases can enter the pore but cannot pass each other anymore in cylindrical pores, and therefore the molecules may have a strong mutual influence on their permeance.

Case V: The pore diameter is about equal to the kinetic diameter of the gas A, resulting in decreased mobility and pore entrance kinetics. Relatively large molecules (B) cannot enter the pore at all. This phenomenon is called *size-exclusion* or *molecular sieving*. This results in an infinite separation factor for A towards B, while permeance is only dependent on the micropore diffusion rate of A. Molecular sieving refers, in its most absolute sense, to the complete blocking of transport of molecules with a certain size or shape and the free passage of smaller or differently shaped molecules. In molecular sieving, the diffusion molecule interacts strongly with the pore well. Molecular sieving will control transport if the order of magnitude of the pore size is 2 to 3 times the molecular diameter.

4. Results and Discussion

4.1. PMDA-Based PIS Precursors (Class I): Effect of Precursor Composition

4.1.1. Gas Permeation Properties

In order to evaluate the molecular sieving capability of C-SiO_2 membranes, gas permeation experiments were carried out to measure the pure component gas permeability through the C-SiO_2 membranes using nitrogen (N_2, 3.64 Å), oxygen (O_2, 3.46 Å), helium (He, 2.60 Å), and carbon dioxide (CO_2, 3.36 Å).

One of the main goals in this study is to study the changes in properties of the precursor composed of carbon-rich (PMDA-ODA) and siloxane-rich (PMDA-PDMS) domain during the pyrolysis. The pyrolysis conditions such as the pyrolysis temperature, the heating rate, and the pyrolysis atmosphere, are important factors in determining the microstructure and gas permeation properties of pyrolytic carbon membranes.

In the present work, it has been observed that the pyrolysis temperature has a marked influence on permeation characteristics of C-SiO_2 membranes. Figs. 2-4 illustrated the He, O_2, N_2 and CO_2 permeability at 25°C for C-SiO_2 membrane prepared at different pyrolysis temperature (600, 800, and 1000°C), respectively. The gas permeabilities of the selected gases were shown to be in the order of He > CO_2 > O_2 > N_2 as shown in Fig. 5. Usually, the permeabilities of small gases through microporous membranes such as

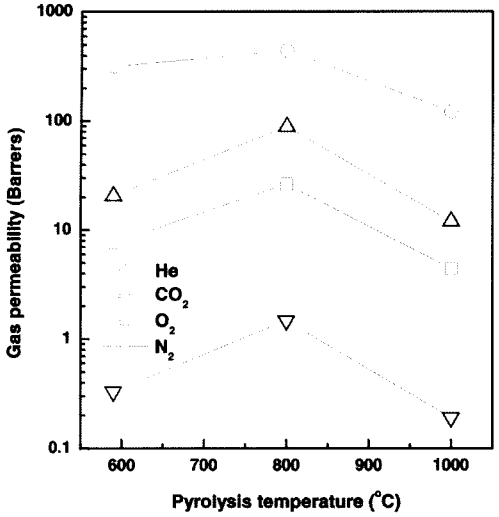

Fig. 2. Gas permeabilities as a function of pyrolysis temperature of C-SiO_2 membrane derived from PIS I.

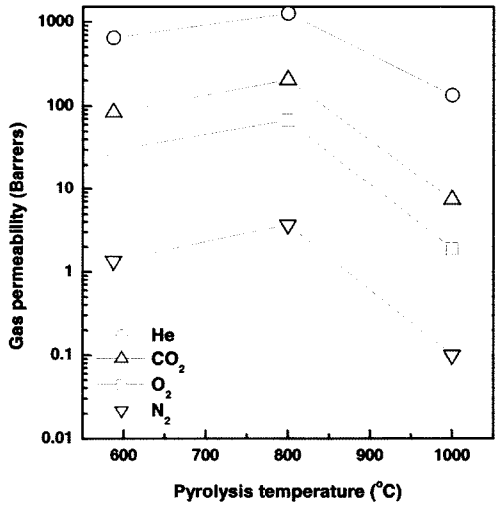

Fig. 3. Gas permeabilities as a function of pyrolysis temperature of C-SiO_2 membrane derived from PIS II.

carbon molecular sieve and/or silica membranes were in agreement with the order of kinetic gas diameter except some peculiar cases. Namely, the gas transport mechanism through these membranes occurred by diffusion-dominant mechanism or size-exclusive mechanism as mentioned above.

All the gas permeabilities increased with the increase of pyrolysis temperature up to 800°C. As

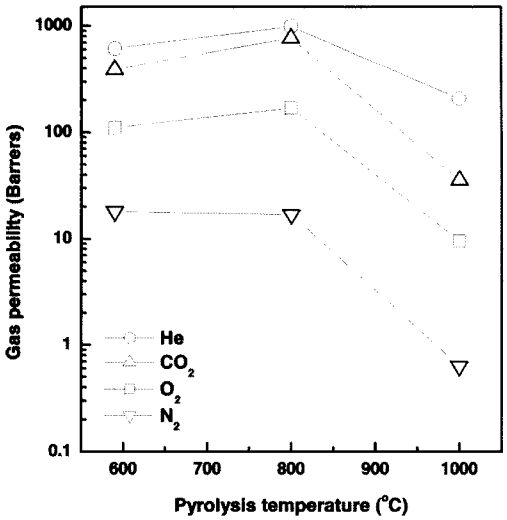

Fig. 4. Gas permeabilities as a function of pyrolysis temperature of C-SiO_2 membrane derived from PIS III.

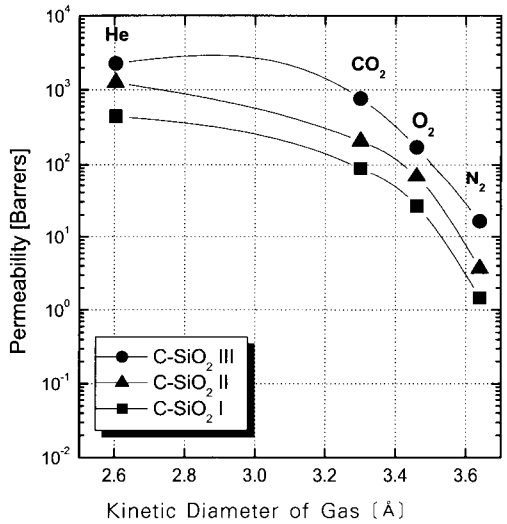

Fig. 5. Gas permeabilities vs. kinetic diameter of gas.

shown in Figs 2-4, the gas permeabilities through C-SiO_2 membrane show a maximum value at 800°C. However, as the pyrolysis temperature increases up to 1000°C, the resulting C-SiO_2 membranes are less permeable than ones pyrolyzed below 800°C. In the case of C-SiO_2 membrane derived from PIS II, the pyrolysis of the polymeric precursor at 1000°C leads to an oxygen permeability of only 2 Barrer in comparison with 68 Barrer at 800°C. This behavior

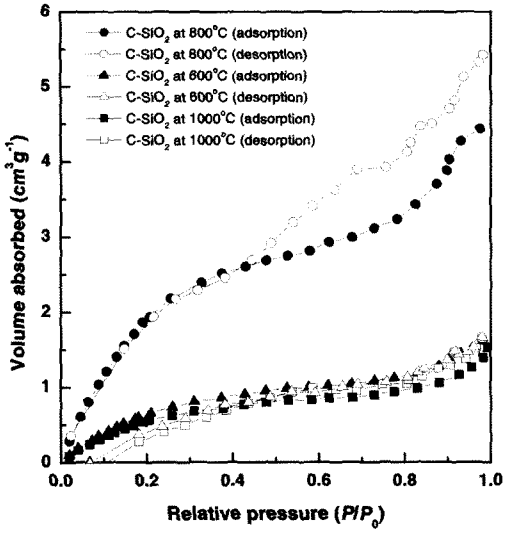

Fig. 6. Nitrogen adsorption isotherms at 77 K of the C-SiO_2 membranes prepared from PIS II precursor.

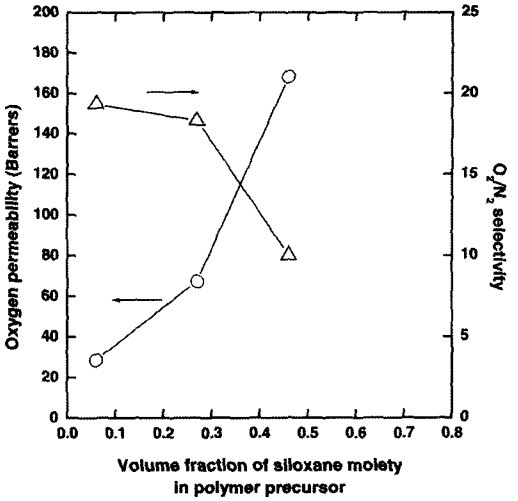

Fig. 7. O_2 permeability and O_2/N_2 selectivity of C-SiO_2 membrane prepared by the pyrolysis at 800°C as a function of the volume fraction of siloxane moiety in the precursor.

was confirmed by nitrogen gas adsorption experiments [BET (Brunauer-Emmett-Teller) method] as shown in Fig. 6.

The volume of nitrogen absorbed in C-SiO_2 membrane prepared at 800°C is greater than those in the C-SiO_2 membranes at 600 and 1000°C. This indicates the formation of transient open pores in the domain of SiO_2-rich network at around 800°C in the continuous carbon matrix. This is in a good agreement with the result from gas permeation experiment. Nitrogen adsorption results of 600 and 1000°C pyrolyzed C-SiO_2 membranes exhibit characteristics of Langmuir (or type I) isotherms, which imply that they are microporous materials. The isotherms of C-SiO_2 membrane pyrolyzed at 800°C shows the adsorption characteristics of type IV. The 800°C isotherm shows that the adsorption undergoes an increase at P/P_0 > 0.7, which indicates that a number of ink-bottle like pores are generated at 800°C. Although the pores in diameters of less than 1.7 nm are not measured, Fig. 6 testifies that the pyrolysis operation both opens up and sinters the pores of C-SiO_2 membrane with pyrolysis temperature.

From the gas permeation and N_2 adsorption experiments, temperatures around 800°C represent an optimum pyrolysis temperature from the standpoint of a permeation rate and a permselectivity. Moreover, this gas permeation behavior upon changing the pyrolysis temperature can be described by the variation in the open porosity of polysiloxane domain versus pyrolysis temperature. Cordelair and Greil[20] recently reported that polysiloxanes $[RSiO_{1.5}]_n$ with R = CH_3 (PMS) and C_6H_5 (PPS), respectively, were transformed to Si-O-C ceramics of variable composition and structure upon pyrolysis in an inert atmosphere at 500-1500°C. They used mercury intrusion measurements to confirm the formation of large transient open pores in the temperature range where thermal degradation occur, and revealed that open porosity (vol%) reached a maximum value at 800°C of pyrolysis temperature in the case of polysiloxane with methyl group. This result is in a good accordance with the maximum gas permeabilities of C-SiO_2 in the present study, assuming that the gas transport could occur preferentially in carbon-poor region, SiO_2 phase.

The O_2 permeabilities and the selectivities of O_2/N_2 of C-SiO_2 membrane prepared at 800°C are represented as a function of initial siloxane content in a precursor matrix in Fig. 7. The gas permeabilities and the selectivities to nitrogen of all the samples are summarized in Table 2. Note that the O_2 permeabilities of C-SiO_2 membranes tend to increase with the

Table 2. Gas Permeation Results of C-SiO_2 Membranes at 25°C

Precursor	Pyrolysis Temperature (°C)	Permeability [Barrer]*				Selectivity to N_2		
		He	O_2	CO_2	N_2	O_2/N_2	CO_2/N_2	He/N_2
PIS I	600	315	7.6	21	0.33	23	62	955
	800	442	27	89	1.47	18.4	61	304
	1000	121	4.5	12	0.19	24	64	643
PIS II	600	1258	30	84	1.35	22.2	62	1033
	800	1393	68	204	3.68	18.5	56	341
	1000	133	2	7.4	0.10	20	74	1330
PIS III	600	610	111	386	18	6.2	21	34
	800	981	168	765	16.8	10	46	58
	1000	207	9.5	36	0.63	15	57	56

* 1 Barrer = $10^{-10} \times cm^3(STP)cm/cm^2 \cdot sec \cdot cmHg$

volume fraction of initial siloxane moiety in original imide-siloxane copolymer matrix, but the O_2/N_2 selectivities decrease from 19 to 10.

It is worthwhile mentioning the gas permeation properties of the polymeric precursor used before pyrolysis, because the microstructure of polymer is closely related with its gas transport behavior. Our previous works on the gas permeation behavior of precursors reported on the transport behavior of rigid-flexible block copolymer membranes such as poly(amideimide siloxane) and poly(imide siloxane) [21,22]. For the polyimides where a siloxane moiety was introduced, the oxygen permeability increased from 1 Barrer to 100 Barrer but the selectivity of O_2/N_2 selectivity decreased from 10 to 2.5 with an increase in the siloxane content. Interestingly, it was observed that the oxygen permeability drastically increased at around 0.2-0.3 volume fraction of siloxane in a copolymer matrix. The percolation concept meaning the formation of effective shortest path around this composition was introduced and applied to explain this behavior. Indeed, the structure of poly(imide siloxane) could be explained by a two phase model with a partial mixed interphase. Unlike block copolymers with well-ordered microphase separated structure, the poly(imide siloxane) is segmented block copolymers where the geometric disorder, that is, random segment size distribution, forces the mixing of the hard (rigid) and soft (flexible) segments. Thus, this randomly ordered two-phase system is very similar to percolating system that two components with different characteristics are randomly mixed. Furthermore, a partial mixed interface between two phases might easily lead to connected phases with a gradual addition of one phase. From these results, it was assumed that the carbonization of these block copolymers with two characteristic domains should lead to the changes of gas permeation properties. Also, the effect of heterophase such as SiO_2 on the gas separation properties of pyrolytic carbon membranes should be seriously considered.

As shown in Fig. 7, the O_2 permeability increased at around 0.3 volume fraction of a siloxane moiety in a precursor, indicating that the characteristic skeleton of two phases might be considerably conserved even after the pyrolysis. Indeed, the rigid imide domain composed of the aromatic backbone and the flexible siloxane domain conducted a role as "organic molecular sieve" and "percolator," respectively. After the transition from the organic to the inorganic phase by the heat treatment, the imide and siloxane domains are gradually changed into "carbon rich" phase with the crosslinked voids of amorphous regions with the interlayer spacing of the graphite-like or highly ordered microcrystalline, and "SiO_2 rich" phase with sparse carbon clusters.

The diffusion coefficients and diffusion selectivity of O_2 and N_2 are summarized in Table 3. The diffusion selectivities of C-SiO_2 membranes are usually higher than those of usual polymeric membranes. The high selectivity of C-SiO_2 membrane is attributed mainly by the increase of diffusion selectivity. Generally, non-

Table 3. O_2 and N_2 Diffusion Coefficients ($cm^2s^{-1}, \times 10^{-9}$) and Diffusion Selectivity of C-SiO_2 Membranes

C-SiO_2		600°C	800°C	1000°C
Class I-1	O_2	1.38	5.82	1.09
	N_2	0.14	0.36	0.11
	$D(O_2)/D(N_2)$	10	15.5	9.9
Class I-2	O_2	4.55	9.48	0.89
	N_2	0.50	0.65	0.10
	$D(O_2)/D(N_2)$	9.1	14.6	8.9
Class I-3	O_2	48.60	10.65	0.62
	N_2	15.00	1.03	0.07
	$D(O_2)/D(N_2)$	3.2	10.3	8.3

porous polymers and molecular sieving matrices such as carbon molecular sieves and zeolites transport gas molecules by a similar sorption-diffusion mechanism. The permeability of a penetrant through a membrane is measured as a steady-state flux, normalized by partial pressure difference and membrane thickness. Permeability of component 'A' can be expressed as the product of a kinetic factor, the diffusion coefficient (D_A), and a thermodynamic factor, the sorption coefficient (S_A):

$$P_A = D_A S_A \quad (2)$$

The ideal permselectivity, $\alpha_{A/B}$, characterizes the overall ability of a membrane to separate penetrants *A* and *B*. This is an inherent property of the material and its molecular geometry. The permselectivity can be factored into a diffusion-selectivity and a sorption-selectivity term as follows:

$$\alpha_{A/B} = \frac{P_A}{P_B} = \frac{D_A}{D_B}\frac{S_A}{S_B} \quad (3)$$

Generally, the sorption-selectivity term for the O_2/N_2 pair lies in the range of 1-2 in almost all glassy polymers, and between 0.7 and 2 for molecular sieving materials like zeolites and a carbon molecular sieve. Therefore, as shown in Table 3, it is the diffusion selectivity in these C-SiO_2 membranes in the present study that is responsible for the remarkable differences in their separation properties.

4.2. BTDA-Based PIS Precursors (Class II): Effect of Phase Geometry

4.2.1. Precursor Morphology

Thermal analysis has been performed to study the

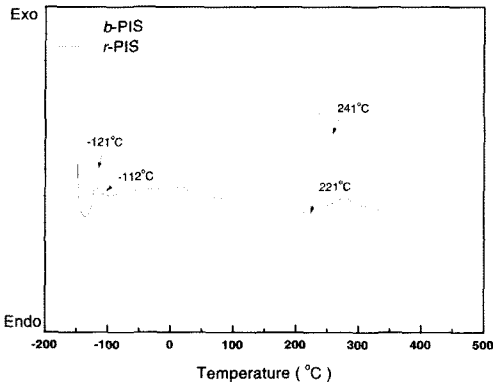

Fig. 8. DSC scans of *b*-PIS and *r*-PIS (N_2 purge, heating rate: 5°C/min).

miscibility of each domain- imide (BTDA-ODA) and siloxane (PDMS) phase in block and random poly (imidesiloxane)s (*b*-PIS and *r*-PIS). In particular, the compatibility between two phases in the solid state is traditionally assessed by examining the number and location of glass transitions (T_g) using thermal analysis techniques. The analysis of DSC thermograms in multiphase polymers was carried out to evaluate the degree of phase separation. Although the degree of phase separation is not quantitatively evaluated by only DSC thermograms, the DSC measurement provides us sufficient informations on compatibility between each phase in multiphase polymers.

Fig. 8 shows the DSC thermograms of *b*-PIS and *r*-PIS films. Because two films are composed of both rigid and flexible domains, two T_gs for each parent polymeric domain were observed at low (T_g of siloxane domain) and high (T_g of aromatic imide domain) temperatures, respectively. For a binary blend or copolymer of amorphous polymers, if a single T_g intermediate between those of the parent polymers is

observed, the mixture is considered to be miscible. If two T_g's identical to those of the parent polymers are observed, then the mixture is considered immiscible. If two T_g's are observed, but are shifted from the parent polymers, then the mixture is multiphase with some intermixing of the polymers.

Since siloxane is nonpolar, microphase-separated copolymers derived from this coblock tend to show high phase purity, whereas the polyimide block is expected to retain the local ordering and orientation, characteristic of the polyimide homopolymer. In DSC study, T_g of siloxane domain in *b*-PIS (-121°C) is very close to T_g of pure siloxane component (T_g of pure PDMS: -123°C), while T_g (-112°C) of siloxane domain in *r*-PIS was upper-shifted. T_g of imide domain in *r*-PIS (221°C) is lower than that of *b*-PIS (241°C). This indicates that *b*-PIS has more phase-separated structure than *r*-PIS, due to the formation of larger siloxane block sequences. In contrast, two phases in *r*-PIS has a broader interface between two phases than those in *b*-PIS and is also more mixed structures. In the PISs investigated in the present study, the domain size of siloxane segment in *r*-PIS might be smaller than that of siloxane segment in *b*-PIS due to the different reactivity ratios of two diamines with BTDA in one-step polymerization. That is, the *r*-PIS will exhibit a multi-block molecular structure, leading to larger intermediate mixed phase than *b*-PIS prepared from two-step polymerization.

Fig. 9 shows TGA thermograms of *b*-PIS and *r*-PIS films under air atmosphere. TGA thermograms of two polymers are very similar to each other. The residual SiO_2 content in two copolymers remained above 700°C is about 11%. From TGA result, it is inferred that two polymers contained nearly the same siloxane content in PIS matrix as intended in synthesis. From DSC and TGA results, we believed that two precursor films might have the same siloxane content but the domain size or building block sequence might not be the same due to the difference in the preparation method.

4.2.2. C-SiO_2 Morphology

Above gas permeation results are very stimulating because the virgin skeleton of two-phase polymeric precursor can be conserved well after the pyrolysis

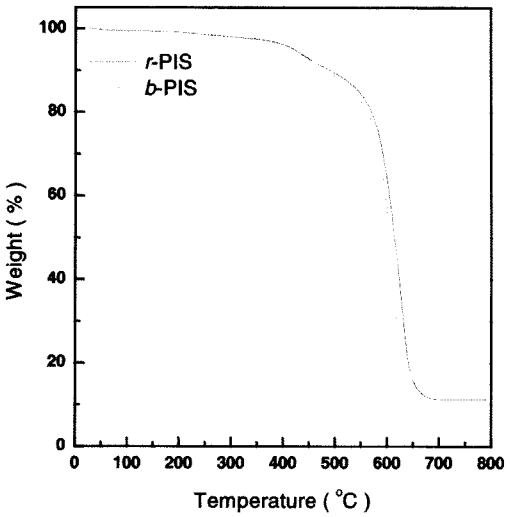

Fig. 9. TGA curves of *b*-PIS and *r*-PIS (air atmosphere, heating rate: 10°C/min)

and carbonization. This might be also achieved by using two thermally stable phases-carbon and silica phases. During the heat treatment, the aromatic imide domain was converted into carbon-rich phase while the siloxane domain was transformed into SiO_2-rich phase. To confirm this assumption, the morphologies of two pyrolytic membranes were observed by using transmission electron microscopy (TEM, JEOL JSF-2000FX JEOL, Inc., MA, U.S.A.). TEM images were taken with 200kV to observe the microstructure of the pyrolytic C-SiO_2 membranes. Samples of the carbon membranes for examination by TEM were prepared by gently scrapping the surface layers of the carbon membranes onto carbon-coated TEM grids using a flesh razor blade. Fig. 10 shows two pyrolytic samples derived from r-PIS and b-PIS membranes. In TEM images, black spot is amorphous carbon-rich phase while white spot is SiO_2-rich phase with a little carbon-poor phase. As can be seen in Fig. 10, two TEM images are very different depending on the microstructures in initial PIS membranes. The formation of larger siloxane domain in b-PIS membrane results in larger SiO_2-rich phase than r-PIS. On the other hand, r-PIS membrane showed well-dispersed microstructure with small siloxane domains in continuous imide matrix when inferred from TEM image after the pyrolysis.

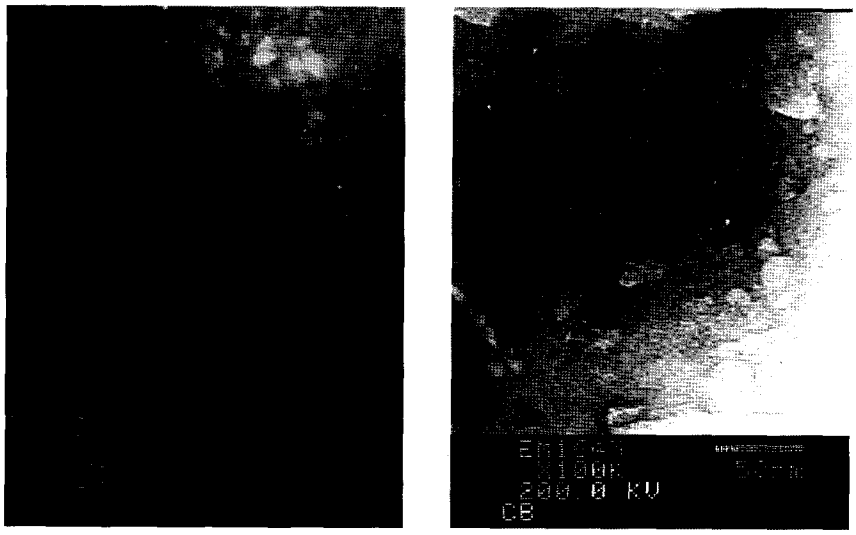

(a) (b)

Fig. 10. TEM images of the pyrolytic carbon-silica membrane pyrolyzed from (a) *r*-PIS and (b) *b*-PIS precursors.

Table 4. Gas Permeabilities (He, CO_2, O_2, and N_2) of Precursors and Their Pyrolytic C-SiO_2 Membranes at 25°C

Gas (kinetic diameter, Å)	*b*-PIS	*r*-PIS	*b*-C-SiO_2	*r*-C-SiO_2
He (2.60)	9.70	6.75	11000	8420
CO_2 (3.30)	3.29	0.93	155	26
O_2 (3.46)	0.94	0.27	55.8	19.3
N_2 (3.64)	0.22	0.06	3.9	0.6

(unit: Barrer, 1 Barrer = 1×10^{-10} cm^3 (STP) cm / cm^2 sec cmHg)

Table 5. Gas Selectivities (He/N_2, CO_2/N_2, and O_2/N_2) of Precursors and Their Pyrolytic C-SiO_2 Membranes at 25°C

Gas pair	*b*-PIS	*r*-PIS	*b*-C-SiO_2	*r*-C-SiO_2
He/N_2	44.1	112.5	2820	14020
CO_2/N_2	15.0	15.5	39.7	43.3
O_2/N_2	4.3	4.5	14.3	32.2

4.2.3. Gas Permeation Properties

It is very important to relate the gas permeability with the morphological change in the heterogeneous polymers such as blends or copolymers. The copolymers with two phases have been investigated in order to improve the gas permeation and separation properties by changing the composition of two phases. Generally, one phase has good mechanical stability and impermeable to gases (but selective to gas pairs) while the other phase has highly permeable to gases. Thus, the proper combination of two phases causes the polymeric membrane to have an improved separation property.

Gas permeation experiments were carried out at 25°C for two PIS membranes and their pyrolytic C-SiO_2 membranes. Gas permeation results for four gases - helium, carbon dioxide, oxygen, and nitrogen and ideal separation factors of other gases to nitrogen are summarized in Tables 4 and 5, respectively. Gas permeabilities of *b*-PIS and *b*-C/SiO_2 membranes were higher for all permeant gases than those of *r*-PIS and *r*-C/SiO_2 membranes.

In this study, we focused on the change of gas permeation properties by morphological changes in copolymers. Although *b*-PIS and *r*-PIS had the same volume fraction of siloxane (0.34), size and sequence

of the more permeable phase, which can be formed differently by the synthesis method, greatly influenced on the gas transport behavior as shown in Table 4. Based on the gas permeation results in Table 4, in the case of *b*-PIS membrane, larger siloxane domains could be formed by two-step polymerization whereas smaller siloxane domains could be formed due to the difference to the reactivity of two diamines by one step polymerization for *r*-PIS membrane. Consequently, this resulted in the discrepancy to the gas selectivities as shown in Table 5 as well as to the gas permeabilities. For O_2/N_2 and CO_2/N_2 separation, *r*-PIS membrane had a little higher selectivities than *b*-PIS membrane, and for He/N_2 separation, *r*-PIS membrane had much higher selectivity than that of *b*-PIS membrane.

It is also interesting to compare the rate of increase for the permeabilities between precursors and their carbonized membranes. For He, the rate of increase in precursor was 1.44, which was very similar to 1.31 in the carbonized membrane. For other gases, the rates of increase in permeabilities were not very different in precursors and their carbonized membranes. For He/N_2, CO_2/N_2, and O_2/N_2 separation, *r*-C-SiO_2 membrane had higher selectivities than *b*-C-SiO_2 membrane. Consequently, these structural differences of pyrolytic membranes resulting from the initial microstructure of precursors led to changes of gas transport behaviors. Thus, it can be concluded that the control of microstructure in two-phase precursor, particularly combined with carbon and silicon, become a most important key factor determining gas separation performance.

5. Conclusions

In class I, we have also found that the C-SiO_2 films obtained at 800°C had higher gas permeability than ones obtained from any other temperatures. This behavior was confirmed by nitrogen gas adsorption experiments [BET (Brunauer-Emmett-Teller) method]. The volume of nitrogen absorbed in C-SiO_2 membrane prepared at 800°C was higher than those in the C-SiO_2 membranes at 600 and 1600°C. This indicated the formation of transient open pores in the domain of the SiO_2-rich network at around 800°C in the continuous carbon matrix. This was in a reasonable agreement

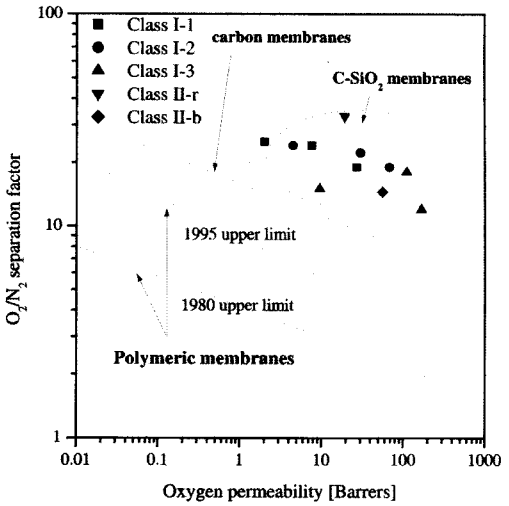

Fig. 11. Oxygen permeability *vs.* oxygen/nitrogen selectivity of the present carbon-silica membranes.

with the result from molecular probe study. In class II, the C-SiO_2 membranes derived from polymeric precursors varying the geometry of random and block sequences in the same composition were prepared. The gas permeation results through these C-SiO_2 membranes exhibited that even the microstructure of phase-separated precursor prevailed in the final structure of the pyrolyzed product. In the meantime, the initial main skeleton of the precursor was considerably conserved after pyrolysis despite of its thermal deformation during pyrolysis. Note that in the polymeric state, class II-b had a higher permeability but lower selectivity than class II-r (class II-b: O_2 (0.94 Barrer, 1 Barrer = 1×10^{-10} cm^3(STP)cm/cm^2 seccmHg) and O_2/N_2 (4.3); class II-r: O_2 (0.27 Barrer) and O_2/N_2 (4.5)).

As illustrated in Fig. 11, O_2 permeability for class I (■, ●, ▲) and class II (▼, ◆) prepared at 600, 800, and 1000oC were plotted versus the best-known reported values, which lay above the dividing line and these results were, to our best knowledge, the highest values in comparison with other gas separation carbon membranes. From this result, we found that the C-SiO_2 membranes have ultramicropore sizes allowing the sieving effect to separate small gas molecules.

We can conclude that the combination of two building blocks with different carbon densities on the nano-scale can provide a hint about a new type of

template carbonization, which differs from the conventional method using thermal stable and thermal unstable phases. Furthermore, the stage has clearly been set for the widespread utilization of a variety of novel C-SiO_2 membranes in a wide range of important application areas.

Acknowledgements

This work is supported by the Korea Institute of Science and Technology evaluation and planning (KISTEP) under the NRL program.

References

1. S. P. Nunes and K.-V. Peinemann, "Membrane Technology in the Chemical Industry," Wiley-VCH, New York, 2001.
2. H. W. Kroto, J. R. Heath, S. C. O'Brien, R. F. Curl, R. E. Smalley, "C60: Buckminsterfullerene," *Nature*, **318**, 162-163 (1985).
3. S. Iijima, T. Ichihashi, "Single-shell carbon nanotubes of 1-nm diameter," *Nature*, **354**, 603-605 (1993).
4. C. R. Bansal, J.-B. Donnet, F. Stoeckli, "Active Carbon," Marcel Dekker, New York, (1988).
5. H. C. Foley, "Carbongenic molecular sieves: synthesis, properties and applications," *Microporous Mater*, **4**, 407-433 (1995).
6. M. B. Shiflett, J. F. Pedrick, S. R. McLean, S. Subramoney, H. C. Foley, "Characterization of supported nanoporous carbon membranes," *Adv. Mater*, **12**, 21-25 (2000).
7. A. B. Fuertes, "Adsorption-selective carbon membrane for gas separation," *J. Membr. Sci.*, **177**, 9-16 (2000).
8. A. Soffer, J.E. Koresh, S. Saggy, US Patent 4,685,940, 11 August (1987).
9. T. A. Centeno, A. B. Fuertes, "Carbon molecular sieve gas separation membranes based on poly (vinylidene chloride-co-vinyl chloride)," *Carbon*, **38**, 1067-1073 (2000).
10. M. B. Shiflett, H. C. Foley, "Ultrasonic deposition of high-selectivity nanoporous carbon membranes," *Science*, **285**, 1902-1905 (1999).
11. H. Kita, H. Maeda, K. Tanaka, K. Okamoto, "Chem. Lett," **179** (1997).
12. T. A. Centeno, A. B. Fuertes, "Supported carbon molecular sieve membranes based on a phenolic resin," *J. Membr. Sci.*, **160**, 201-211 (1999).
13. H. Suda, K. Haraya, "Gas permeation through micropores of carbon molecular sieve membranes derived from Kapton polyimide," *J. Phys. Chem.*, B **101**, 3988-3994 (1997).
14. C. W. Jones, W. J. Koros, "Carbon molecular sieve gas separation membranes-I. preparation and characterization based on polyimide precursors," *Carbon*, **32**, 1419-1425 (1994).
15. Y. Kusuki, H. Shimazaki, N. Tanihara, S. Nakanishi, T. Yoshinaga, "Gas permeation properties and characterization of asymmetric carbon membranes prepared by pyrolyzing asymmetric polyimide hollow fiber membrane," *J. Membr. Sci.*, **134**, 245-253 (1997).
16. J. Ozaki, W. Ohizumi, N. Endo, A. Oya, S. Yoshida, T. Iizuka, "Preparation of platinum loaded carbon fiber by using a polymer blend," *Carbon*, **35**, 1676-1677 (1997).
17. T. Kyotani, "Control of pore structure in carbon," *Carbon*, **38**, 269-286 (2000).
18. M. Inagaki, "New Carbons," Elsevier, New York, (2000).
19. H. B. Park, I. Y. Suh, Y. M. Lee, "Novel pyrolytic carbon membranes containing silica phase: Preparation and characterization," Chem. Mater. in press (2002).
20. J. Cordelair, P. Greil, "Electrical conductivity measurements as a microprobe for structure transitions in polysiloxane derived Si-O-C ceramics," *J. Eur. Ceram. Soc.*, **20**, 1947 (2000).
21. H. B. Park, S. Y. Ha, Y. M. Lee, "Percolation behavior of gas permeability in rigid-flexible block copolymer membranes," *J. Membr. Sci.*, **177**, 143-152 (2000).
22. S. Y. Ha, H. B. Park, Y. M. Lee, "Percolational effect of siloxane content in poly(amideimide siloxane) on the gas permeation behavior," *Macromolecules*, **32**, 2394-2396 (1999).